Proceedings World Geothermal Congress 2005
Antalya, Turkey, 24-29 April 2005

Petrophysical Properties of Fresh to Mildly Altered Hyaloclasitie Tuffs

Julia Frolova (1), Vladimir Ladygin (1), Hjalti Franzson (2) Omar Sigurðsson (2), Valgardur Stefánsson (3), and Vladimir Shustrov (4)

(1) Moscow State University, Geological Department, Russia

(2) Iceland GeoSurvey, 9 Grensásvegur, 108 Reykjavík, Iceland

(3) National Energy Authority, 9 Grensásvegur, 108 Reykjavík, Iceland

(4) JSC "Gazprom" Podzemgasprom Ltd, Moscow, Russia

skalka@geol.msu.ru

Keywords: hyaloclastite, petrophysical properties, Iceland, palagonitization

ABSTRACT

In Iceland a significant part of reservoir rocks of cold and thermal systems are basaltic hyaloclastite tuffs. Hyaloclastites are dominantly formed in sub-glacial eruptions. They are fragmental and glassy rocks as they are formed during a rapid magma quenching in the glacial melt water. Hyaloclastites are highly permeable due to their clastic and very porous structure and should therefore be an important source rock for both thermal and fluid systems. It is known that the capacity and longevity of a reservoir is greatly controlled by the petrophysical properties of the host rocks. The purpose of the paper is to describe the progress results of a petrophysical study of hyaloclastites. About 80 samples of hyaloclastites were collected in the Neovolcanic zone and upper Quaternary rocks of S and SW Iceland and then analyzed with respect to chemical and mineral composition and structure (thin- and polished sections, X-Ray and microprobe analysis) and petrophysical properties among which are density, effective and total porosity, hygroscopy, gas permeability, sonic velocity, axial strength and magnetic characteristic. The petrophysical analysis done to date shows extremely variable characteristics: density (1,2-2,34 g/cm^3), hygroscopy (0,4-13%), porosity (14-57%), permeability (10^{-3}-6,4*10^3 mD), axial strength (1,8-111 MPa), V_p (0,9-4,05 km/sec), magnetic susceptibility (0,3-39 10^{-3} SI). Statistical calculation of data including cluster analysis was done and correlation between petrophysical parameters was estimated. The wide dispersion of properties appears to be highly dependent on the alteration of the hyaloclastites. Basaltic glass is a highly sensitive material and reacts relatively rapidly in cold and hot groundwater environments resulting in chemical and mineral alteration, progressive consolidation and significant changes of petrophysical characteristics. The mineralogical studies allow a classification of alteration stages to be defined - from fresh or slightly palagonized to altered hyaloclastites with zeolites and clay minerals developed in intra-fragmental space and partially in glass. Mineral alteration is correlated with consequent petrophysical changes. The paper considers also the compaction and consolidation of hyaloclastites during regional burial process. A progressive increase in density, sonic velocity and strength and a decrease in permeability occur during gradual burial and increasing age although some exceptions are found.

1. INTRODUCTION

Porosity and permeability are the most important parameters with regards to the potential of cold and hot groundwater systems and the utilization of these resources. The study of these parameters has been ongoing in Iceland for the last decade or so (e.g. Sigurdsson et al. 2000, Franzson et al. 2001) where petrophysical properties have been studied in igneous rock samples of variable composition and hydrothermal alteration. This research project focuses on the particular rocktype hyaloclastite commonly found in Iceland, and which is the source rock for significant part of the groundwaters in Iceland. The project is based on the cooperation between Russian and Icelandic geoscientists as indicated by the list of authors, and this paper describes the first results mainly gathered by the former.

The paper first gives the environment of sampling and followed by a summary of the petrophysical and geological characteristics of the samples. The relations between the different variables are discussed and conclusions reached on their interrelationships.

2. GEOLOGICAL SETTING AND SAMPLING

Iceland sits astride the Mid-Atlantic ridge, and is thus almost totally composed of igneous rocks of which about 90% are basaltic in composition. Most of the eruptives are lava flows except during periodically occurring glacials in the last 3 m.y., when hyaloclasties are formed during eruptions into the glacial meltwater.

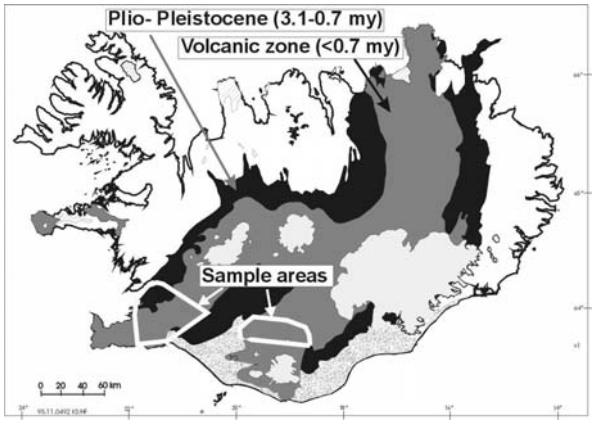

Figure 1. Simplified geological map of Iceland showing volcanic and Plio-Pleistocene zones. The sampling areas in SW and S-Iceland are also shown.

The rock samples were mainly fine grained tuffs, in order to maintain a relative homogeneity between the many sub-samples that had to be taken for the various measurements for each sample. The samples were about 2 cm wide cores drilled from the rocks, were the length was up to 15 cm. An attempt was made to select the sampling sites with respect to

various environments in which the tuffs were deposited (e.g. airfall, foreset bedded, avalance, reworked and mudflows). Secondly, samples were selected with respect to variable alteration or up to the stage that all glass was altered. Of special interest was to sample tuffs that had suffered variable degree of palagonitisation.

3. ANALYTICAL METHODS

3.1 Petrophysical measurements

Petrophysical analysis includes the following determinations: bulk density (ρ), specific density (ρ_s), total porosity (P), effective (connected) porosity by air (P_{air}), water absorption (W), effective porosity by water (P_w), hygroscopic moisture (W_g), gas permeability, velocity of longitudinal waves in dry (V_p) and water-saturated (V_{pw}) environments, strength (uniaxial compression) (R_c), magnetic susceptibility (χ) (Table 1).

Table 1. List and number of petrophysical measurements

Properties		Number of measurements
Bulk density		74
Specific density		63
Total porosity		62
Effective porosity by air		64
Water absorption		72
Effective porosity by water		72
Hygroscopic moisture		63
Gas permeability		24
Velocity of longitudinal waves	Dry	72
	Water saturated	53
Strength		62
Magnetic susceptibility		72
Petrographic analysis		75
X-Ray analysis		9+2
Microprobe analysis		6 samples (42 points)

Standard methods (Trophimov and Korolev, 1993) and plug samples (H=>D=2,5 cm) were used for majority of petrophysical measurements.

Bulk density was defined by standard measurement of geometry and weight of the sample.

Specific density (mineral density of rock) was measured for rock powder on exclusive device ELA (Kalachev *et al*. 1997). The main principle of this device is the law of Boil-Moriotte (pressure*volume=const in isothermal environment). Accuracy is 0.02 g/cm^3.

Then, *total porosity* of rock was calculated as following:

$$P=\{(\rho - \rho_s)/ \rho_s\}*100 \quad (1)$$

where ρ – bulk density, ρ_s – specific density

Effective (connected) porosity by air was defined by ELA for plug samples. The total volume of hard part of the sample with inner closed pores was obtained from the test. Then the effective porosity was calculated. For the calculation it is necessary to know the bulk density of rock.

Water absorption was determined by water saturation during 7 days and the following weighing procedure.

$$W=\{(m_2-m_1)/m_1\}*100 \quad (2)$$

where m_1, m_2 are mass of dry sample, mass of water-saturated sample after 7 days keeping in water, respectively.

Then an *effective (connected) porosity by water* was calculated:

$$P_w=\rho*W \quad (3)$$

Hygroscopic moisture was defined after drying the powder in a thermal safe (T=107^{0}C, 24 hours):

$$W_g=m_1-m_2/m_2 \quad (4)$$

where m_1, m_2 are mass of air-dry powder, mass of absolutely dry powder, respectively.

Gas permeability was measured accordingly with state standard requires (State Standard 1985).

Velocity of longitudinal waves was measured by ultrasonic method (DUK-6B – frequency 700 kHz and US-13 I – frequency 1 MHz) in air-dry and water-saturated environments. On the base of the difference of those values coefficient Q_{vp} was calculated:

$$Q_{vp}= \{(V_{pw} - V_p)/V_p\}*100 \quad (5),$$

where V_p - velocity of longitudinal waves for dry samples, V_{pw} - velocity of longitudinal waves for water-saturated samples.

Petrophysical parameter Q_{vp} helps to study characteristic features of rocks pore-space structure. High value Q_{vp} indicates microfractures and open pores within the rock. Value about nought is the evidence of dense structure with small pores. Negative value indicates presence of clay or other loose secondary minerals, which recompact contacts within rocks under water-saturation (Ladygin and Frolova 2001).

Strength (axial compression) was defined by German hydraulic press CDM-10/91 for plug samples.

Magnetic properties of rocks were characterized by magnetic susceptibility, determined by the Magnetic Susceptibility Meter (Kappameter KT-5).

3.2 Statistic analysis

Statistic analysis was used for petrophysical database proceeding (software "SATISTICA"). Correlation relationships between petrophysical characteristics were studied. Cluster analysis was implemented. There were 8 variables in the base of the cluster subdivision – density, specific density, porosity, effective porosity by air, effective porosity by water, hygroscopy, velocity of longitudinal waves, uniaxial strength. All variables were standardized before clustering:

Std. Value = (Variable - Mean of Variable) / Std. Deviation

K-mean type of cluster analysis was selected for hyaloclastite clustering. This program starts with k random clusters, and then moves objects between those clusters with the goal to minimize variability within clusters and maximize variability between clusters. Casewise deletion of missing data was chosen so that only cases, which did not contain any missing data for any of the variables, selected for the analysis, were included in the analysis.

3.3 Petrography and geochemistry

Petrophysical properties were analyzed along with composition and structure of the rocks. All samples were described macroscopically, and then studied in thin sections with transmitted light polarizing microscope and polished section with reflected light microscope.

Mineral composition was identified using by DRON-6 diffractometer. The total spectrum was obtained in a θ range up to 60 ^{0}. Then in order to precise clay mineral types the measurements were done for glycolated powders and after heating at 500 ^{0}C (θ range is 2-30 ^{0}).

Electron microscopy with microprobe analysis was made for portion of the samples (Camebax SX-50).

4. RESULTS AND DISCUSSION

4.1 Petrography and structure of hyaloclastites

The rocks studied represent subglacial basaltic hyaloclastite sequence of Pliocene-Pleistocene age developed widely in Iceland. They are clastic glassy rock composed mainly of angular, vesicular, isotropic grains of volcanic glass cemented by secondary authigenic minerals. Crystaloclasts of olivine, pyroxene and plagioclase develop in a small amount. The grain size of studied samples varies in a range 0,01-1 cm.

The six samples taken for microprobe analysis show an olivine-tholeiite composition. Chemical composition of volcanic glass is given in Table 2.

Basaltic glass is a thermodynamically unstable material, which is very sensitive to alteration. It reacts relatively rapidly with cold or hot groundwater entailing chemical and mineral alterations. All hyaloclastites studied are altered to some degree but the magnitude of alteration varies significantly from one sample to another. The first product of glass alteration is so-called palagonite. Term palagonite is commonly used for any hydrous alteration product of mafic glass and also for crystalline material evolving from palagonite itself (Peacock, 1926; Moore, 1966; Hay and Iijima, 1968; Furnes, 1975; Heptner, 1977; Zhou and Fyfe, 1989; Thorseth et.al., 1991; Stroncik and Shmincke, 2001). Two main types of palagonite are usually distinguished: 1) yellow, isotropic, clear “gel palagonite” and 2) yellow-brown, slightly anisotropic, birefringent, fibrous palagonite, which develops during more advanced steps of palagonite on the outer surface of gel palagonite. Many papers describe palagonitization of volcanic glass and offer various mechanisms of palagonite formation. It is accepted by the majority of geologists, that some type of dissolution-precipitation process is responsible for the alteration of basaltic glass to palagonite. At the same time some authors suggest that palagonite is residual hydrated product replacing the glass and that the dominant loss of elements occur in a solid state due to diffusion, prior to a partial network dissolution of the glass (Hay and Iijima, 1968; Crovisier et.al, 1987, 1992; Stroncik and Shmincke, 2001).

Palagonite is a typical material for all samples studied but its amount is quite variable. Basically, palagonite develops on the surface of glass grains, around vesicles and along the fractures. In general, the chemical composition of palagonite and parent glass differs significantly from each other. Moreover, palagonite forms zonal rinds around glassy grains and vesicles, which can be chemically and texturally different. The general variation of chemical composition along glass-palagonite profile is clearly shown in the diagrams (Figure 2**).**

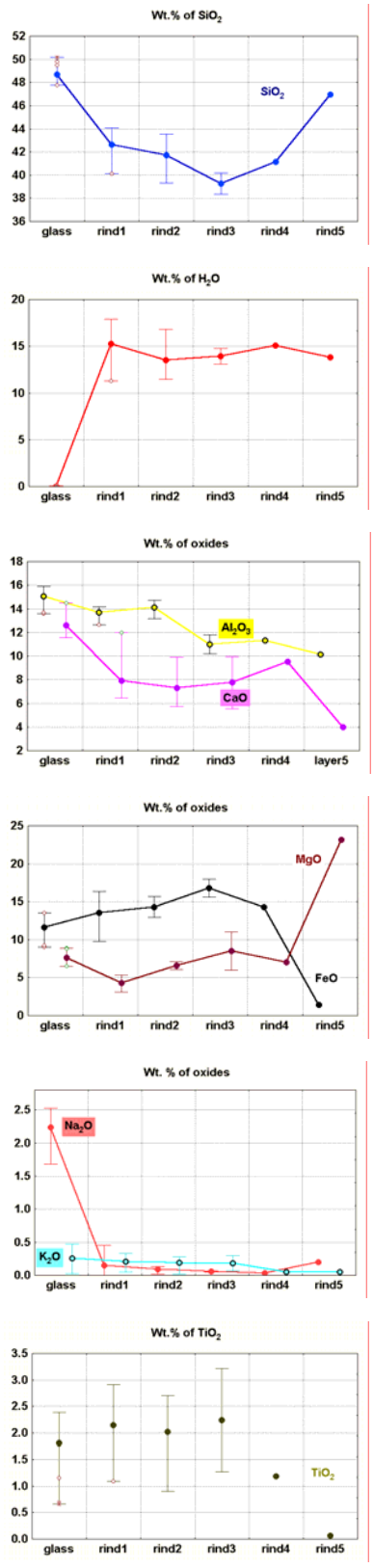

Figure 2. Chemical variation along a glass-palagonite profile (microprobe data).

Relative to the parent glass, the palagonite shows a reduction in SiO_2, Al_2O_3, CaO, Na_2O, an increase in FeO (except the outermost rind) and variable concentrations of TiO_2 MgO wt.% content shows uncertain tendency, increasing remarkably in the outermost rind. Major element totals of palagonite vary from 82 to 88 wt.%. The difference to 100 wt.% is balanced by the water content, as has been

concluded by Stroncik and Shmincke (2001), based on the results of infrared photometer analysis.

The character of the boundary between glass and palagonite is variable. Sharp boundary is observed in the majority of samples (Figure 3A). In this case the central part and the edge of the glassy grain have a similar chemical composition. In a number of samples the gradual boundary between glass and palagonite can be observed with sign of glass edge leaching. Some samples are characterized by dendritic structure of palaganite/glass front (Figure 3B). Dark dendritic branches extend into fresh glassy grains. According to Crovisier et.al. (1992) sharp/gradual or dendritic alteration fronts may reflect rapid or slow alterations rates, respectively. Microfractures, which are formed at the palagonite-glass boundary due to their physical dissimilarity are pathways for fluids and subsequent alteration.

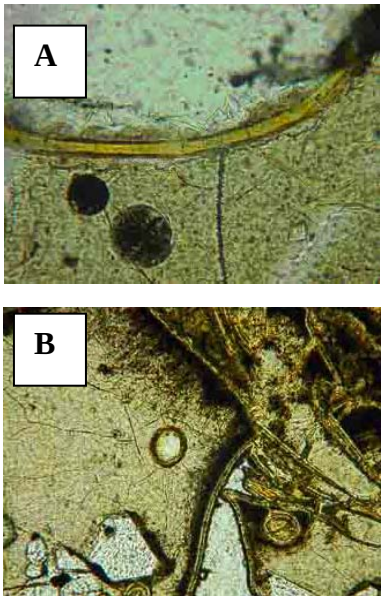

Figure 3. Thin section images in plane-polarized light showing the main boundary types between glass and palagonite. Width is 0,9 mm. (A) Sharp boundary; (B) Dendritic boundary

Palagonitization is responsible for the first cementation of glassy grains into consolidated rocks. Extensive palagonitization is usually associated with authigenic mineralization – mostly zeolites, clays and calcite, which develop in inter granular space and pores. The general cross section through the most altered hyaloclastite contains the following zones: fresh glass core, gel-palagonite rind, laminated palagonite rind, clay minerals and zeolites. Detailed petrographical and geochemical studies (thin sections, X-ray, SEM) allow a classification of alteration stages to be defined - from fresh or slightly palagonized to altered hyaloclastites with zeolites and clay minerals developed in intra-fragmental space and partially in glass. Their description and correlation with petrophysical properties will be given below.

4.2 Petrophysical properties of hyaloclastites

4.2.1. General characteristic

Petrophysical properties of hyaloclastites vary extensively. Distribution of the main petrophysical characteristics is shown in histograms (Figure 4). Bulk density varies from 1,20 to 2,34 g/cm^3. Specific density, which reflects mineral composition of rock, changes from 2,45 to 3,07 g/cm^3, while the most common value is 2,7-2,9 g/cm^3 that conforms to basaltic composition. Hyaloclastites are very heterogeneously porous and permeable. They can be extremely porous and permeable (up to 57% and 6,4*10^3 mD, respectively) as well as having low porosity and permeability (14% and 1*10^{-3} mD, respectively). Hygroscopic moisture, which depends on clay or amorphous minerals content (especially smectite and palagonite), varies from 0,4 up to 13%.

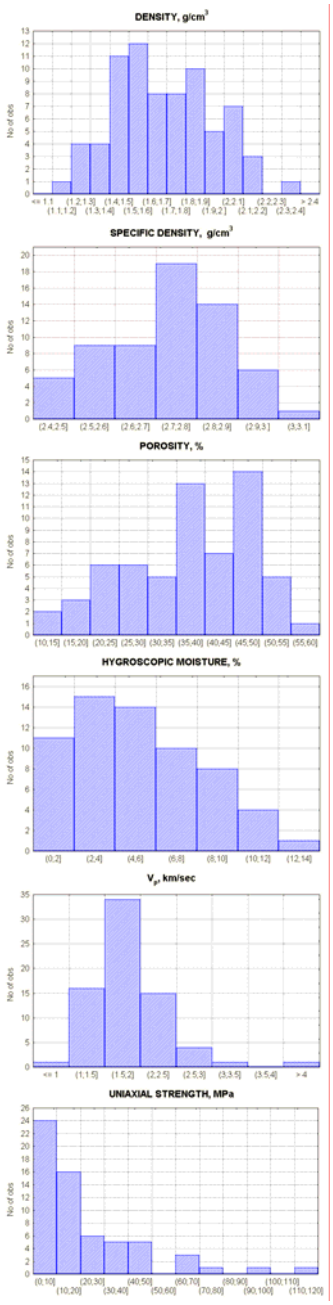

Figure 4. Histograms showing petrophysical properties of hyalolastites.

Sonic velocity varies between 0,9-4,05 km/sec and changes in water saturated environment up to 1,15-4,3 km/sec. Parameter Q_{vp}, showing how sonic velocity changes after saturation by water, lies in a range –10 – +156 %. Negative Q_{vp} value indicates a velocity decrease after water saturation, which is basically due to the destruction of clay contacts between grains, while the high positive Q_{vp} value is a result of significant velocity increase. The strength of hyaloclastites is very variable, which is measured to change

from 1,8 up to 111 MPa. The limit of magnetic susceptibility variability is 0,3-39*10^{-3} SI.

4.2.2 Petrophysical groups obtained by cluster analysis

In order to understand the nature of properties variability and define petrophyiscally homogeneous groups a cluster analysis was done. Groups obtained by cluster analysis were correlated with geological factors among which were petrography, secondary alteration, age and depth of burial. Five groups (clusters) were obtained by cluster analysis. Petrophysical properties of each cluster are shown in Table 3 and box plots (Figure 5). The characteristic features of each group are described below.

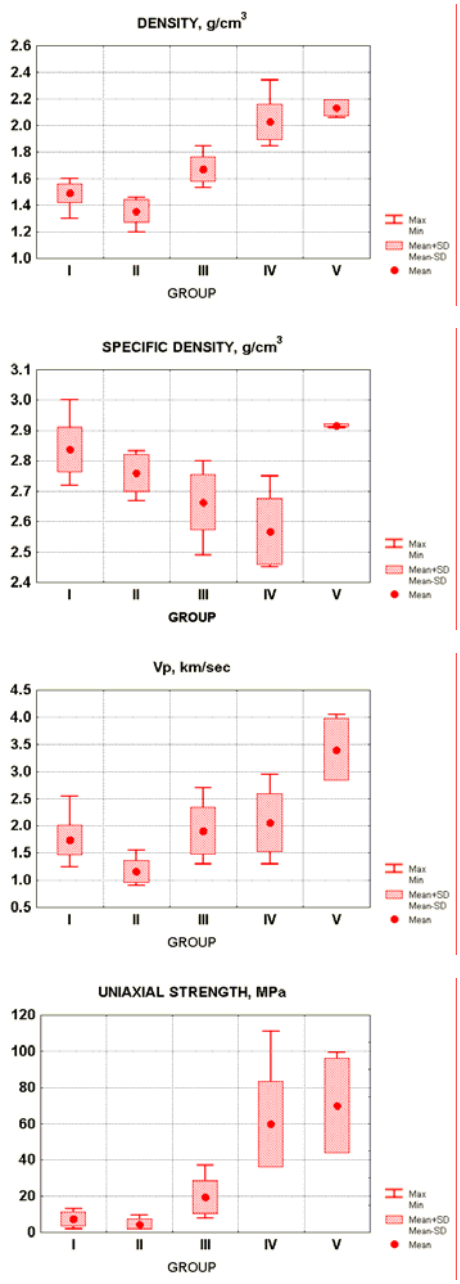

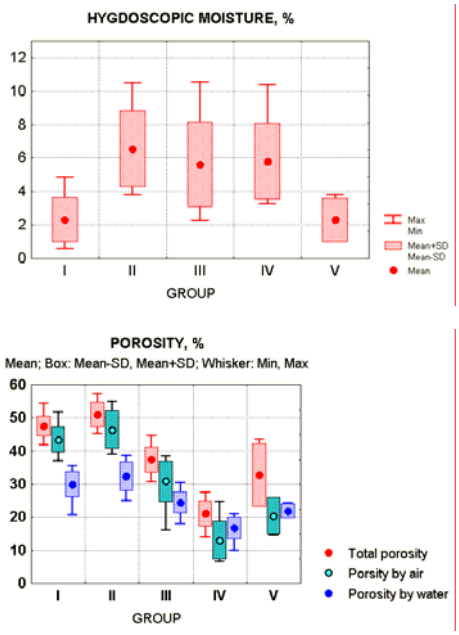

Figure 5. Petrophysical properties of hyaloclastites by groups I-V (clusters)

Group I.

Petrographically this group comprises the most fresh and only slightly cemented hyaloclastites, which have been formed during the last glacial period and have never been affected by burial process. The rocks of this group are mostly dark brown, and only rarely yellowish brown.

The samples of this group represent the first stage of palagonitization. Glass grains are fresh or only slightly altered form the edge by palagonitization process. Thin palagonite rinds (up to 5, rarely 10 micron) occasionally develop on the grain surface. Formation of the first contact cement between grains is shown in Figure 6.

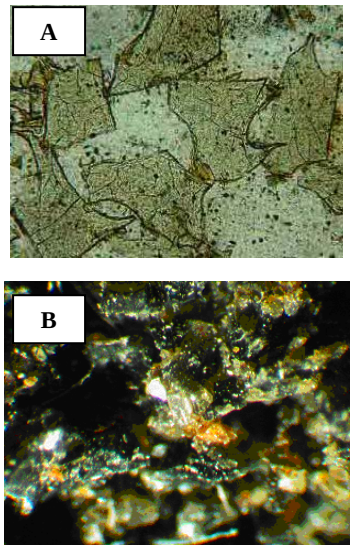

Figure 6. Representative hyaloclastite of Group I. (A) Thin section view in plane-polarized light. Glassy grains fused on contacts by amorphous material. Width is 0.9 mm; (B) Polished section view in reflected light. Black glassy grains cemented by yellow palaganite along contact.

Cementation of gassy grains has occurred due to fusion of the amorphous material (palagonite) along contacts between grains. Glassy grains as well as material developing on contacts are optically isotropic when studied in thin sections. XRD analysis doesn't show any crystalline secondary minerals; only amorphous substance is identified.

Microprobe analysis shows no difference between central part and edge of glassy grain (Figure 7, Table 4).

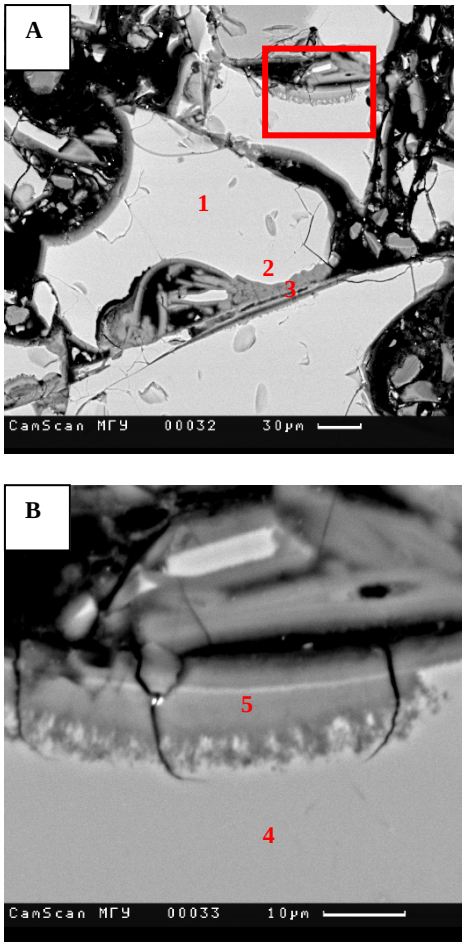

Figure 7. Electron microscope images of representative hyaloclastite of Group I. View of contact cementation composed of gel-palagonite between glass grains. The first stage of palagonization. Numbers: 1. Glass core; 2. Glass edge; 3. Contact material; 4. Glass core; 5. Palagonite rind. See text for further explanation.

Palagonite derived from glass shows considerable reduction in SiO_2, MgO, CaO and Na_2O; slight losses of Al_2O_3, FeO and K_2O, and a slight increase of TiO_2. The boundary between glass and palagonite is mainly sharp. In some cases the zone of glass leaching (2-3 microns thick) is observed along internal surface of glassy grain (Figure 7B). Microfractures are developed perpendicular to the glass/palagonite alteration front.

Hyaloclastites of Group I have low density (ρ=1,3-1,6 g/cm^3, average 1,49 g/cm^3), high porosity (P=41,8-54,4%, average 47,5%) and permeability ($2*10^2$-$6*10^3$ mD, average $3,3*10^3$ mD) that is a result of primary composition, clastic structure and empty inter granular pores. Effective porosity by air (P air=36,9-51,7%, average 43,4%) is quite similar to total porosity. Almost all pores are connected (Pair/P=0,8-1). Effective porosity by water is on average 30% lower in comparison with effective porosity by air. Hygroscopic moisture is characterized by relatively low value, varying in a range 0,6-4,87% (average 2,3%) that is explained by a very small amount of palagonite and an absence of clay minerals. Hyaloclastites are only slightly cemented resulting in a low strength value (2-13 MPa, average 7 MPa) and low sonic velocity (1,25-2,5 km/sec, average 1,75 km/sec).

Group II

Hyaloclastites of II group are quite similar to the first group but characterized by more pronounced alteration. Initially dark brown rocks change their color into bright yellow, where the light yellow is due to increased palagonitization. Glassy grains are coated with palagonite rinds, averaging 10 microns in thickness (do not exceed 20 microns), forming filmy cementation (Figure 8). Palagonite develops around vesicles within glassy grains as well. Palagonite rinds are mainly optically isotropic in polarized light although slightly anisotropic outer rinds are observed in some cases. Intergranular space remains empty.

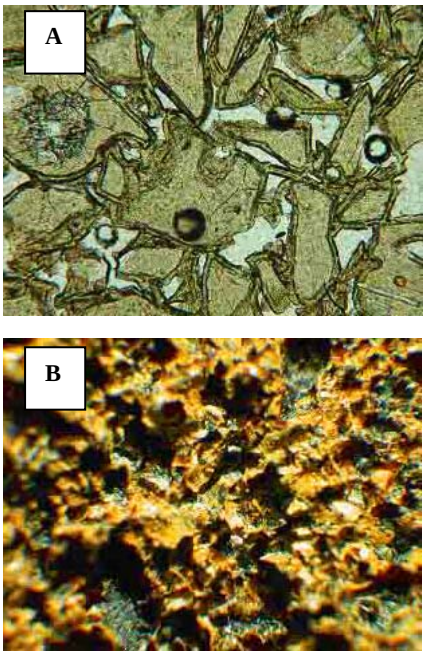

Figure 8. Representative hyaloclastite of Group II. (A) Thin section view in plane-polarized light. Filmy cementatation of glass grains by gel-palagonite rinds. Width is 0,9 mm. (B) Polished section view in reflected light. Black glassy grain coated and cemented by palagonite.

Among all rocks studied, hyaloclastites of Group II are the most porous (45,3-57,3%, average 50,9%), extremely permeable (1,7-$6,4*10^3$ mD) and characterized by the lowest density (1,2-1,46 g/cm^3, average 1,35 g/cm^3). A slight decrease of bulk and specific density and an increase of porosity and permeability are observed in comparison with the previous group (Figure 5). This tendency indicates that alteration process develops as a substitution of glass edges by palagonite rather than a simple precipitation of palagonite on the surfaces of glassy grains without glass alteration. According to Hay and Iijima (1968) the density of palagonite is about 1,93-2,14 g/cm^3, while the density of fresh basaltic glass is 2,75-2,85 g/cm^3. This leads to the conclusion that substitution of volcanic glass by porous, low

dense palagonite and the absence of secondary material in inter granular space entails a reduction of total hyaloclastite density and increasing of porosity during this stage of alteration. Effective porosity by air is quite similar to total porosity; almost all pores remain connected (Pair/P=0,8-0,96). Effective porosity by water is by 30% (in average) lower in comparison with effective porosity by air. Hygroscopic moisture of hyaloclastites greatly increases at this stage up to 3,81-10,5% (average 6,54%) that is related to the palagonite development. Hyaloclastites remain slightly cemented and characterized by the lowest strength (1,8-9,7 MPa, average 4,4 MPa) and sonic velocity (0,9-1,55 km/sec, average 1,15 km/sec).

Group III

Majority of the hyaloclastites representing Group III belong to the last glaciation and have not been buried, while some samples are of 2 m.y. age and have been buried down to 700-1000 m. Hyaloclastites are basically yellowish in color. The surface of glassy grains and walls of vesicles are covered by rinds of palagonite: inner layer is composed of optically isotropic gel-palagonite and outer layer – of anisotropic laminated palagonite (Figure 9).

Small vestibules (diameter less than 0,05 mm) are totally filled by palagonite while large ones (larger than 0,1 mm) have empty central parts. Inter granular space is filled by palagonite or the mix of palagonite and smectites (Figure 10). Microprobe analysis done for sample of considered group shows only slight reduction in SiO_2, Al_2O_3, MgO and a significant loss in Na_2O and oxides totals during palagonitization (Table 5).

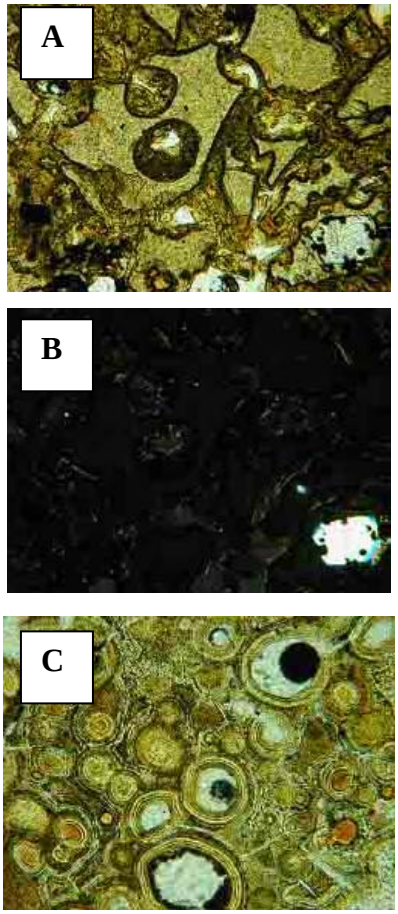

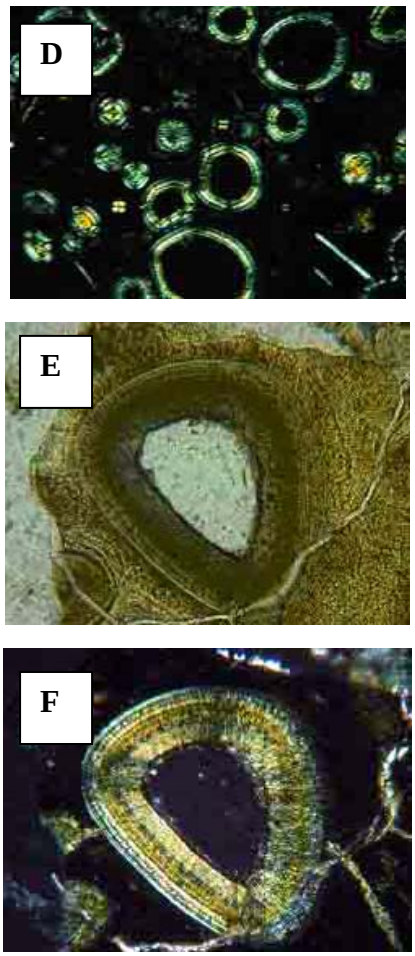

Figure 9. Thin section images. Representative hyaloclastites of Group III with cementation of intergranular (porous) type. (A, B) General view of hyaloclastite, with inter granular cement, slightly anisotropic (in plane- and cross polarized light, respectively). Width of images is 0,9 mm; (C, D) View of vesicles, with several generations of palagonite rims (in plane- and cross polarized light, respectively). Small pores are totally filled; large pores are empty in central parts. Width of images is 0,9 mm; (E, F) Enlarged view of palagonite rims around vesicle (in plane- and cross polarized light, respectively). Width of images is 0,35 mm.

The filling of intergranular space and the formation of porous cement results in the increase of density (1,53-1,85 g/cm^3, average 1,67 g/cm3), sonic velocity (1,3-2,7 km/sec, average 1,9 km/sec) and strength (7,6-37 MPa, average 19 MPa) and as a consequence a reduction of porosity (30,6-44,6, average 37 %) and permeability (0,4-9,5*10^2 mD, average 6,1*10^{2}mD) (Figure 5). The difference between total porosity, effective porosity by air and effective porosity by water is observed for considered alteration stage. Effective porosity by air approximately 20% lower compared with total porosity, while 20% higher, than effective porosity by water. Thus, some reduction of a number of effective pores (relatively total number of pores) is observed on this stage. Intensive development of palagonite and smectite causes high hygroscopy (2,24-10,55 %, average 5,59%) and a significant reduction of specific density (2,49-2,8 g/cm^3, average 2,66 g/cm^3).

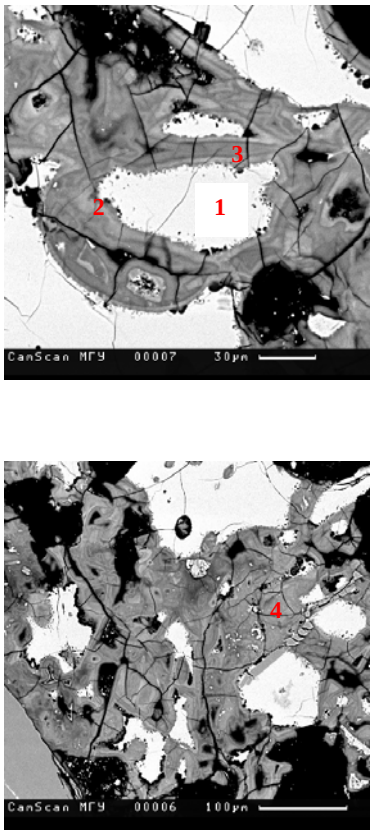

Figure 10. Electron microscope images of representative hyaloclastite of Group III. Intergranular (porous) type of cementation with palagonite. Numbers: 1. Glass core; 2. Inner rind; 3. Outer rind; 4. Inter granular material

Group IV

This group joins particoloured hyaloclastites of different age (from last glaciation to 1,7-2 m.y.) and burial depth (from no burial to 700 m). A characteristic feature of hyaloclastites, belonging to Group IV, is the occurrence of several generations of palagonite and intergranular authigenic minerals – zeolites, calcite and smectites (Figure 11**).**

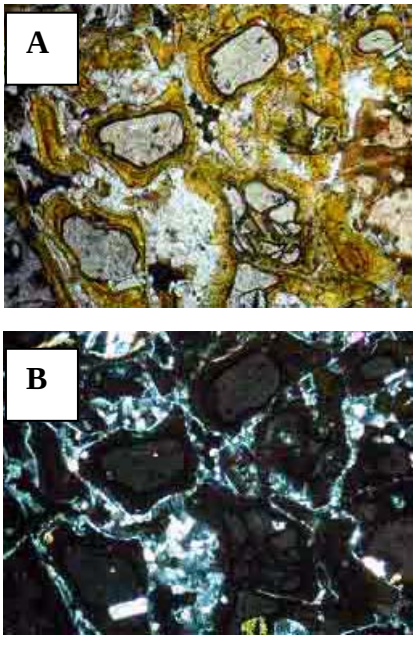

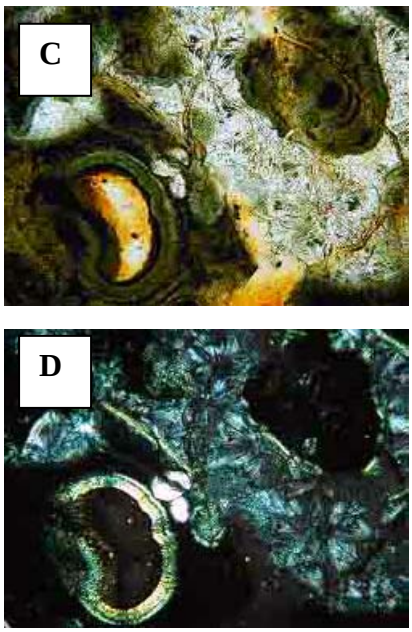

Figure 11. Thin sections images of representative hyaloclastites from Group IV: in plane- (A,C) and cross-polarized (B,D) light. Photos show filmy cementation with palagonite and porous cementation with palagonite, zeolite and smectites. Width is 0,9 mm.

Palagonite developed consists both of isotropic and anisotropic types. Obviously, palagonite is partially re-crystallized into smectite. Presence of smectites is confirmed by X-ray analysis. Detailed investigation of clay material reveals that it is trioctahedral smectite or mixed-layered smectite-chlorite with prevalence of a smectite component. Zeolites developing in fractures and intergranular space are rhombs of chabasite and radial-axial aggregates of phillipsite (Figure 11). XRD analysis reveals Ca-zeolites garronite and levine as well.

Intergranular space is almost totally filled by authigenic minerals. Glass grains remain partially fresh although vesicles are filled with zeolites or clays. Fractures through glass grains are observed to provide paths for fluids (Figure 12).

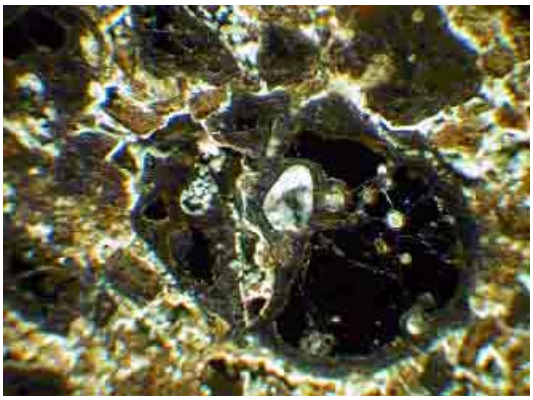

Figure 12. Polished section image in reflected light. Unaltered glass core, palagonite rinds, vesicles and intergranular space filled by zeolites. Width is 1 mm.

Chemical variations through parental glass, palagonite substituting glass and material covering vesicles are shown in Figures 13, and 14. A reduction of SiO_2, Na_2O, MgO, and CaO along with an increase in FeO, TiO_2 and H_2O is

observed during two steps of palagonitization (points 2 and 3 in Figure 14). In the third rind of palagonite (point 4 in Figure 14) SiO_2, Na_2O continue to diminish while TiO_2 and FeO continue to increase; the amount of Al_2O_3 is lowered, while MgO increases in comparison with parent glass. Microprobe analysis reveals that the rims around vesicles (points 5 and 6) are composed of Ca-zeolites as seen by high amount of SiO_2, Al_2O_3 and CaO.

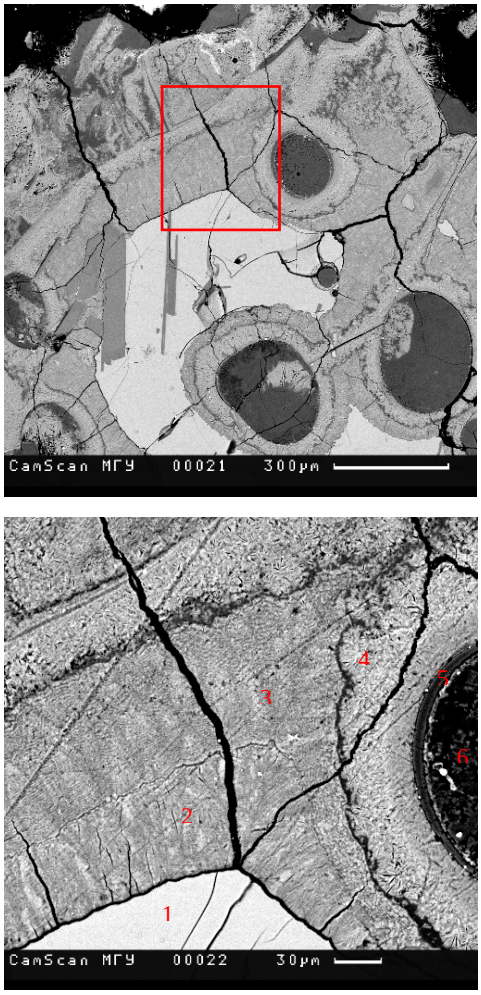

Figure 13. Electron microscope image. 1. Fresh glass core; 2. 1st rind of palagonite; 3. 2 d rind of palagonite; 4. Outer rim around vesicle; 5. Inner rim around vesicle; 6. Zeolite in vesicle.

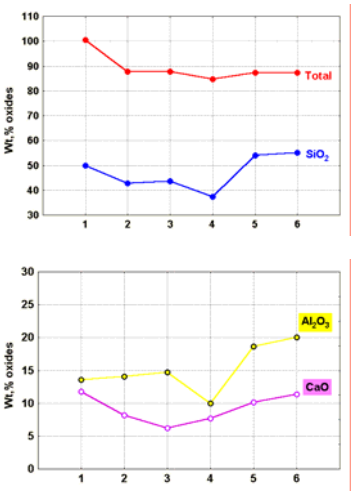

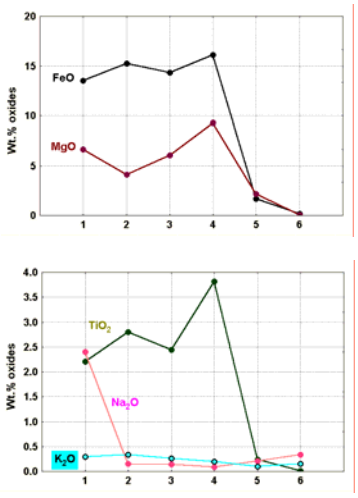

Figure 14. Microprobe analyses through palagonite and parental glass along the profile shown in Figure 13.

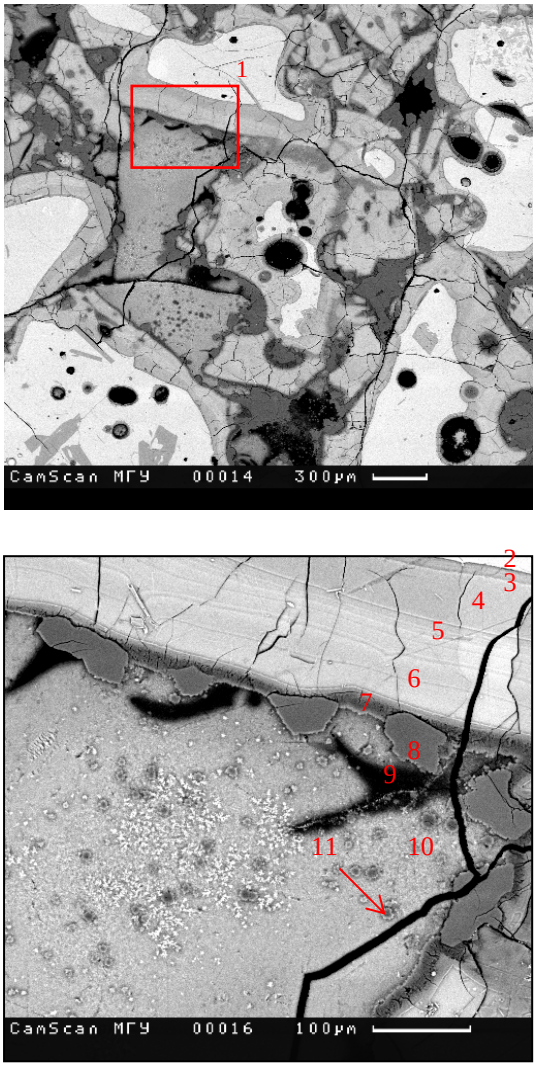

Figure 15. Electron microscope images. 1. Fresh glass core; 2. Glass edge; 3. 1st rind of gel palagonite; 4. 2d gel palagonite rind; 5. 3d laminated palagonite rind; 6. 4th laminated palagonite rind 7. 5th outermost rind; 8 Grain of zeolite; 9. Authigenic minerals in pore; 10. Intergranular material; 11. "Dark spots" within intergranular material

Another profile is presented in Figures 15 and, 16. There the central part of the glassy grain and the edge are chemically similar (points 1 and 2). During palagonitization (points 3-7) SiO_2, Al_2O_3, CaO, Na_2O and MgO are depleted while H_2O, TiO_2 and FeO increase. The outermost layer (point 7) is characterized by a sharp increase of MgO. Crystals of zeolites develop along the boundary between palagonite and the intergranular material. (point 8). Chemical composition confirms an analcime. The intergranular material is likely to be zeolites or a mixture of zeolites and clay minerals (points 9-11).

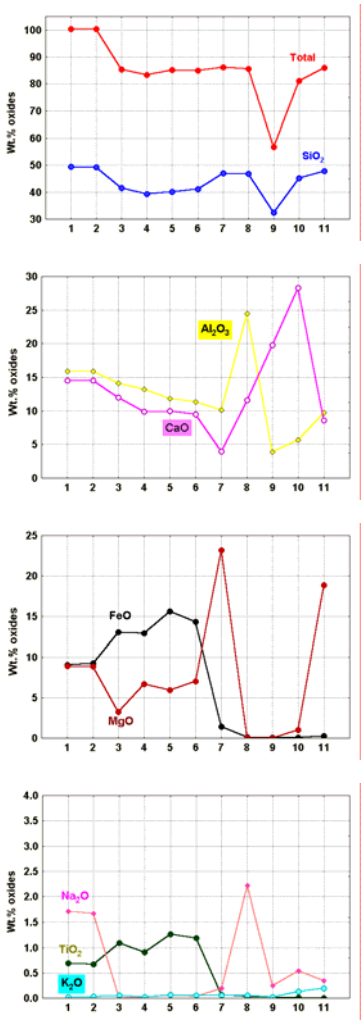

Figure 16. Representative microprobe analyses of palagonite and parental glass along profile shown in Figure 15.

Hyaloclastites of Group IV are significantly denser (1,85-2,34 g/cm^3, and on average 2,03 g/cm^3) and mechanically stronger (40-111 MPa, on average 60 MPa) in comparison with previous groups (Figure 5, Table 3). Intensive development of authigene minerals in intergranular space and pores causes a considerable reduction of porosity (14-27,5%, average 21%) and permeability (0,23-203 mD, average 55 mD). Effective porosity by air is notably lower in comparison with total porosity. Only about 60% of all pores remain connected.

Another characteristic feature of this group is an unusual ratio between P_{air} and P_w: effective porosity by air is similar or even lower than effective porosity by water. It appears that an explanation of this unusual fact is the wide development of smectite, which is characterized by special microstructure. From one side smectite is able to absorb a great amount of water in its structure resulting in an increase of P_w, but from the other side it is impermeable for air.

A wide development of smectite results in the high hygroscopy varying in a range 3,25-10,4% (average 5,79%). Specific density is characterized by the lowest values (2,45-2,75 g/cm^3, average 2,57 g/cm^3) due to high degree of basaltic glass alteration and development of zeolites with low specific density (2,1-2,2, g/cm^3). Sonic velocity is not much higher (1,3-2,95 km/sec, average 2,05 km/sec) in comparison with previous groups in spite of relatively low porosity and high density. A wide zeolites occurrence is assumed to be the reason of low velocity. It has been shown in previous studies of zeolitic tuffs from Kamchatka that intensive zeolitization entails significant reduction of sonic velocity (Ladygin et.al. 2000)

Group V.

This group represents strongly consolidated light grey color hyaloclasites 2-2,5 m.y. age, which have been buried down to the depth about 1000 m and are furthest from the volcanic zone. Hyaloclastites are altered to a high degree. Intergranular space, fractures and vesicles are filled by authigene minerals (Figure 17A,B). In contrast to previous group glass grains are altered considerably (Figure 17C,D). The main second minerals are chlorite or corrensite, calcite, clinozoisite, prehnite, quartz.

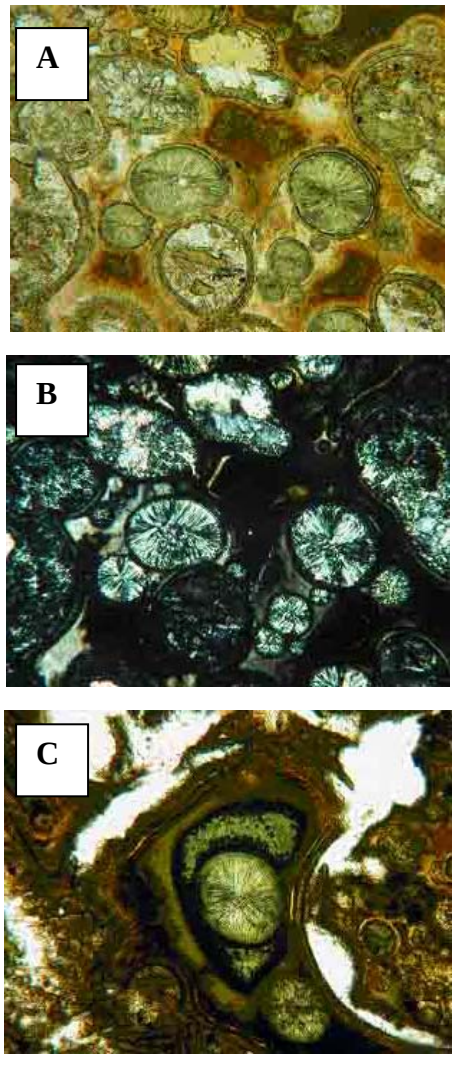

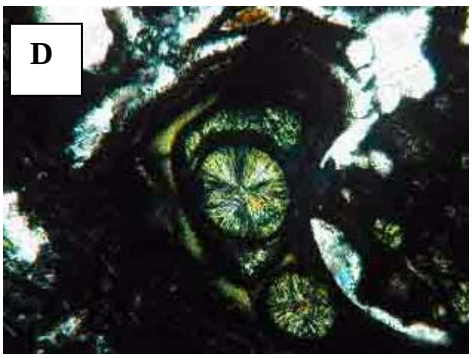

Figure 17. Thin section images of Group V hyaloclastite in plane- (A,C) and cross-polarized (B,D) light. Vesicles are filled by chlorite or corrensite and calcite. Width is 0,9 mm.

These are the most dense (2,06-2,18 g/cm^3, average 2,13 g/cm^3), impermeable (10^{-3}-6*10^{-2} mD) and strongest (48-00 MPa, average 70 MPa) rocks with the highest sonic velocity (2,95-4,05 km/sec, average 3,4 km/sec) in spite of some increasing of total porosity in comparison with previous group (Figure 5, Table 3). It appears that second porosity has been formed during intensive substitution of volcanic glass by corrensite, which has ultra-small pores, impermeable to fluids.

A ratio P_{air}/P shows that similar to previous group about 60% of all pores is connected. An unusual ratio $P_{air}/P_w \leq .1$ similar to previous alteration group is typical for considered stage as well.

Gradual transformation of smectites into chlorite results in significant hydroscopy decreasing down to 2,29% in average (1,48-3,8 %). Specific density reflecting mineral composition becomes as high as 2.92 g/cm^3 due to development of second minerals among which are chlorite, calcite, clinozoisite.

4.2.3 Relationship between petrophysical properties

Correlation between total and effective porosity. Line plot (Figure 18) illustrates correlation between total porosity, effective porosity by air and effective porosity by water. It can be seen that for high porosity values the following correlation is typical:

$$P>=P_{air}>>P_w$$

Almost all pores are open for air but water can't penetrate to small pores so that is characterized by lower values. Different correlation is typical for the interval of low porosity values (< 20%):

$$P=>P_w>P_{air}$$

It is highly unusual to observe that effective porosity by air is lower than effective porosity by water. In order to understand this feature, low porous samples were studied in detail. Petrographic analyses show that these samples contain abundant clay minerals. XRD analysis shows that the clays are smectite or mixed layered smectite-chlorite (corrensite). It is known that smectite can absorb a great amount of water in its structure and swells out. Obviously, the significant amount of smectite explains satisfactorily the unusual correlation shown above. Smectite is on one hand impermeable to air, while on the other absorbs a great amount of water, which shows up as an increase of P_w.

Correlation between other petrophysical properties. High correlation exists between permeability and porosity as shown in Figure 19A. The general tendency of permeability decrease with increasing age and burial depth is observed in the scatter plot. However, the most ancient and altered hyaloclastites has the lowest permeability (10^{-3}-6*10^{-2} mD) in spite of relatively "mid range" porosity values. Apparently a secondary porosity has been formed during glass transformation at this alteration stage. This porosity is typical for corrensite and characterized by ultra small size, and impermeable for fluids.

Close correlation is observed between permeability and uniaxial strength **(**Figure 19B**)**. It appears that formation of strong, dense contacts and cementation between glassy grains and gradual filling of intergranular space by secondary minerals during alteration process results in increasing strength and decreasing permeability.

Correlation between V_p and ρ is shown in Figure 19C. Zeolitized hyaloclastite samples of Group IV do no correlate well with the general trend as in spite of having relatively high density they are characterized by low V_p values. As mentioned above the zeolite abundance is assumed to be the reason for the low velocity.

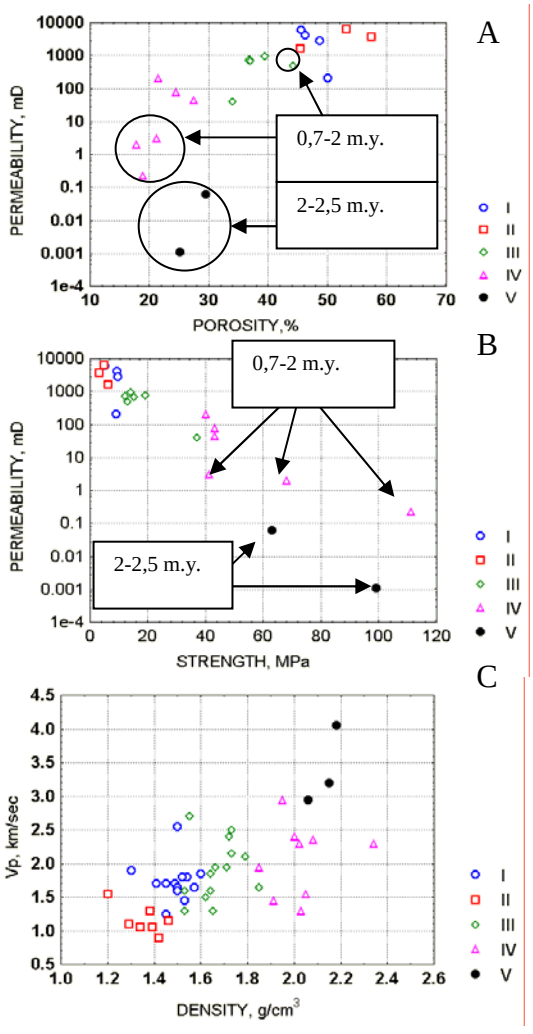

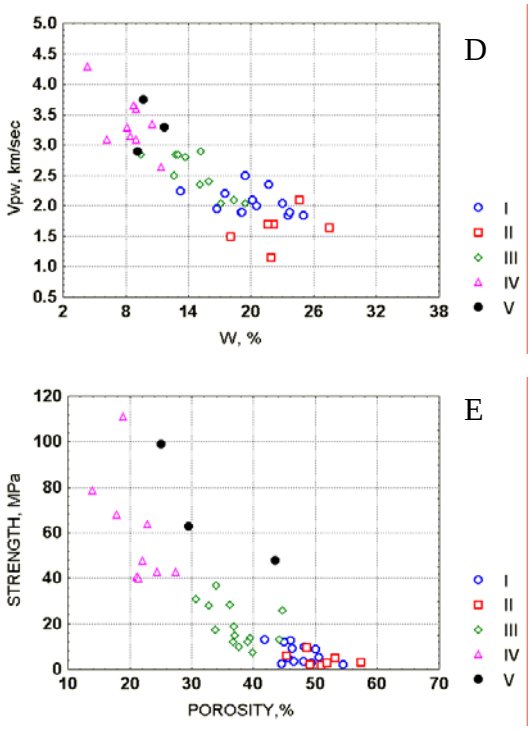

Figure 19. Relationship between petrophysical properties of different groups.

High correlation is found between V_{pw} and W (Figure 19D). Relationship between strength and porosity is characterized by a good correlation, although ancient chloritized hyaloclastites of Group V are out of the common tendency being stronger in comparison with other hyaloclastites (Figure 19E).

CONCLUSION

1. Alteration products in studied hyaloclastites show the following evolution: gel-palagonite - laminated palagonite - smectite and zeolites – corrensite/chlorite, calcite, prehnite, clinozoisite.

2. Alteration process entails the gradual change of cement types: contact – filmy - porous – secondary porous/basal and with intensive re-crystallization of primary material. Palagonite is responsible for the first cementation of loose volcanic deposits and its transformation into consolidated rock.

3. Petrophysical properties of hyaloclastites are characterized by wide dispersion that appears to be highly dependent on the types and degree of alteration. This wide dispersion reveals that the hyaloclastites can form both aquifers as well as water confining horizons.

4. Petrophysical properties correlate with the stage of alteration, burial depth and age of hyaloclastites. The most porous, permeable and weakly rocks are hyaloclastites at an initial stage of alteration (when gel-palagonite substitutes the edge of glassy grains and forms contact-filmy cement) from last glaciation, which have not been buried. The strongest and most consolidated rocks are hyaloclatites of 2-2,5 m.y., which have been buried down to 1 km. They are intensively altered with chlorite, calcite, clinozoisite, prehnite and in spite of a formation of a secondary porosity they remain the lowest in permeability.

5. Intensively altered, relatively low porous (<20%) hyaloclastites are characterized by an unusual $P_{air}/P_w \leq 1$ ratio which is believed to result from a wide development of clay minerals (smectite, corrensite), which are impermeable for air but are able to absorb a great amount of water.

NOMENCLATURE

ρ–bulk density, ρ_s specific density, P - total porosity, P_{air} - effective (connected) porosity by air, W - water absorption, P_w - effective porosity by water, W_g - hygroscopic moisture, V_p - velocity of longitudinal waves, V_{pw} – velocity of longitudinal waves in water-saturated environment, R_c - strength (axial compression), χ – magnetic susceptibility.

ACKNOWLEDGMENTS

This research was financially supported by a NATO grant from Icelandic Research Council and Russian Foundation for Basic Research (grant 05-03-64842). We are grateful to Dr. Shlykov V.G. and Dr. Krivokoneva D. for X-ray analysis, to Kononkova N. for microprobe analysis.

REFERENCES

Crovisier J.L., Honnorez J., and J.P. Eberhart, Dissolution of basaltic glass in seawater; mechanism and rate, *Geochim. Cosmochim. Acta*, 51(11), 2977-2990, 1987

Crovisier J. L., Honnorez J., Fritz B., and Petit J.-C.: Dissolution of Subglasial Volcanic Glasses from Iceland: Laboratory Study and Modelling, *Applied Geochemistry*, Suppl.Issue 1, 55-81, 1992

Franzson H., Gudlaugsson S. Th., and Fridleifsson G. O. Petrophysical properties of Icelandic rocks. *Proc. 6th Nordic Symposium on Petrophysics*, 1-14, 2001

Furnes H.: Experimental palagonitization of basaltic glasses of various composition, *Contrib.Mineral.Petrol.*, 50, 105-113, 1975

Hay R.L, and Iijima A.. : Nature and Origin of Palagonite Tuffs of the Honolulu Group on Oahu, Hawaii, *Geol.Soc.Amer. Met.* 116, 338-376, 1968

Heptner A.P.: Palagonite and palagonitization process, *Lithology and mineral resources*, 5, 113-129, 1977

Jercinovic M.J., Keil K, Smith M.R., and Schmitt R.A.: Alteration of Basaltic Glasses from North-Central British Columbia, Canada, *Geochimica et Cosmochimica Acta*, Vol. 54, 2679-2696, 1990

Kalachev V., Volovik M., and Ladygin V.: Express method for Definition of Rock Specific Density, *Bulletin of Moscow State University*, Series 4, N 2, 51-56, 1997

Ladygin V., Frolova J, and Rychagov S.: Formation of Composition and Petrophysical Properties of Hydrothermally Altered Rocks in Geothermal Reservoir, *Proceeding of the World Geothermal Congress 2000*. Japan. 2695-2699, 2000

Ladygin V.M. and Frolova J.V: The stages of volcanic rocks petrophysical properties alteration during the Earth evolution, *Proceedings 6-th Nordic Symposium on Petrophysics.* Nordic Petroleum Technology Series VI, Electronic version, 2001

Moore. J.G.: Rate of palagonitization of submarine basaltadjacent to Hawaii, *U.S.Geol.Surv.Prof.Pap.*, 550-D, D163-D171, 1966

Peacock M.A.: The petrology of Iceland, Part 1, The basic tuffs, *R. Soc.Edinburgh,Trans*., 55, 53-76, 1926

Schiffman P., Spero H.J., Southard R.J., and Swanson D.A.: Control on Palagonitization versus Pedogenic Weathering of Basaltic Tephra: Evidence from the Consolidation and Geochemistry of the Keanakako'i Ash Member, Kilauea Volcano, *Geochemistry, Geophysics, Geosystems* – An Electronic Journal of the Earth Sciences, vol. 1, 2000

Sigurdsson O., Gudmundsson A., Fridleifsson G. O., Franzson H., Gudlaugsson S. Th., and Stefansson V.: Database on Igneous Rock Properties in Icelandic Geothermal Systems. Status and Unexpected Results. *Proc. World Geothermal Congress*, 2881-2886. 2000

State Standard of Russian Federation. Rocks. Method of Determination of Absolute Gas Permeability Coefficient under Stationary and Non-stationary Filtration. *GOST 26450.2-85. State Committee of USSR by Standards*, 1985

Stroncik N.A., and Shmincke H-U.: Evolution of Palagonite: Crystallization, Chemical Changes, and Element Budget, *Geochemistry, Geophysics, Geosystems* – An Electronic Journal of the Earth Sciences, vol.2, 2001

Thorseth I.H., Furnes H., and Tumyr O.: A Textural and Chemical Study of Iceland Palagonite of Varied Composition and its Bearing on the Mechanism of the Glass-Palagonite Transformation, Geo*chim. Cosmochim Acta*, 55, 731-749, 1991

Trophimov V.T., and Korolev V.A.: The Methods of Rock's Properties Investigation. *Practicum by Soil Geology*, 168-333, 1993

Zhou Z., Fyfe W.S.: Palagonitization of Basaltic Glass from DSDP Site 335, Leg 37: Textures, Chemical Composition, and Mechanism of Formation, *American Mineralogist*, Vol. 74, 1045-1053, 1989

Table 2. Chemical composition of volcanic glass (microprobe data)

	SiO_2	TiO_2	Al_2O_3	FeO	MgO	MnO	CaO	Na_2O	K_2O	SO	ClO	Total
15--8	47.777	2.327	15.227	12.326	7.178	0.243	12.082	2.374	0.390	0.000	0.046	99.969
15--3	48.812	2.382	15.183	11.713	7.098	0.205	11.550	2.496	0.473	0.010	0.034	99.959
17--10	49.501	0.689	15.917	9.039	8.889	0.132	14.487	1.715	0.024	0.000	0.028	100.420
20--10	48.521	1.398	15.922	10.837	8.370	0.119	13.084	2.154	0.145	0.022	0.079	100.651
20--10	49.405	1.338	15.777	10.581	8.362	0.142	12.832	2.099	0.124	0.017	0.049	100.726
22-13	49.796	2.205	13.579	13.523	6.636	0.121	11.773	2.398	0.289	0.017	0.172	100.511
22-13	50.181	2.230	13.678	13.059	6.485	0.138	11.669	2.523	0.275	0.000	0.132	100.370

Table 3. Petrophysical characteristic of hyaloclastites groups (clusters)

	I cluster (14 samples)	II cluster (7 samples)	III cluster (14 samples)	IV cluster (9 samples)	V cluster (3 samples)
Density, g/cm^3	1,3-1,6 1,49	1,2-1,46 1,35	1,53-1,85 1,67	1,85-2,34 2,03	2,06-2,18 2,13
Specific density, g/cm^3	2,72-3 2,84	2,67-2,83 2,76	2,49-2,8 2,66	2,45-2,75 2,57	2,91-2,92 2,92
Hygroscopy, %	0,6-4,87 2,3	3,81-10,5 6,54	2,24-10,5 5,59	3,25-10,4 5,79	1,48-3,8 2,29
Total porosity, %	41,8-54,4 47,5	45,3-57,3 50,9	30,6-44,6 37,3	14-27,5 21,1	25,1-43,4 32,7
Effective porosity by air%	36,9-51,7 43,4	39,1-55 46,4	16-38,4 30,8	6,5-24,8 13	14,5-25,5 20,4
Pair/P	0,81-1 0,91	0,81-0,96 0,91	0,52-0,96 0,82	0,33-0,9 0,61	0,49-0,87 0,64
Effective porosity by water, %	20,7-35,5 29,9	25-38,7 32,3	18-30,4 24,4	9,9-20,9 16,7	20-24,3 21,9
Permeability, mD	(0,21-5,98)*10^3 3,33*10^3	(1,68-6,35)*10^3 3,9*10^3	(0,4-9,53)*10^2 6,08*10^2	0,23-203,8 55,45	10^{-3}-6*10^{-2} 3*10^{-2}
V_p, km/sec	1,25-2,55 1,75	0,9-1,55 1,15	1,3-2,7 1,9	1,3-2,95 2,05	2,95-4,05 3,4
V_{pw}, km/sec	1,85-2,5 2,05	1,15-2,1 1,65	2,05-2,9 2,5	2,65-4,3 3,35	2,9-3,75 3,3
Q_{vp}, %	-3-40 20	38-62 45	0-56 28	25-156 79	-9-13 1
Strength, MPa	2-13 7,2	1,8-9,7 4,4	7,6-37 19	40-111 60	48-99 70

Table 4. Chemical composition of glass and associated palagonite along profiles shown in Figure 7 (microprobe data)

	SiO_2	TiO_2	$Al2O_3$	FeO	MnO	MgO	CaO	Na_2O	K_2O	SO	ClO	Total
1. Glass core	48,521	1,398	15,922	10,837	0,119	8,370	13,084	2,154	0,145	0,079	0,022	100,651
2. Glass edge	48,159	1,304	15,529	10,964	0,128	8,726	12,46	2,202	0,208	0,0183	0,24	100
3. Contact material	44,097	1,613	13,789	9,772	0,221	5,316	7,277	0,055	0,065	0,019	0,038	82,262
4. Glass core	49,405	1,338	15,777	10,581	0,142	8,362	12,832	2,099	0,124	0,049	0,017	100,726
5. Palagonite rind	45,832	1,68	14,016	9,578	0,134	5,08	8,729	0,262	0,123	0,042	0	85,476

Table 5. Chemical composition of glass and associated palagonite according to Figure 10 (microprobe data).

		SiO_2	TiO_2	$Al2O_3$	FeO	MnO	MgO	CaO	Na_2O	K_2O	SO	ClO	Total
1	Glass core	48,812	2,382	15,183	11,713	0,205	7,098	11,550	2,496	0,473	0,034	0,01	99,959
2	Inner rind	47,798	4,142	14,071	11,3	0,021	4,165	5,660	0,057	0,179	0,006	0	87,398
3	Outer rind	47,185	2,073	14,486	10,954	0,123	5,976	4,589	0,09	0,294	0,022	0,003	86,796
4	Inter granular material	47,685	2,475	14,664	10,952	0,181	4,905	4,567	0,24	0,51	0,034	-	86,212

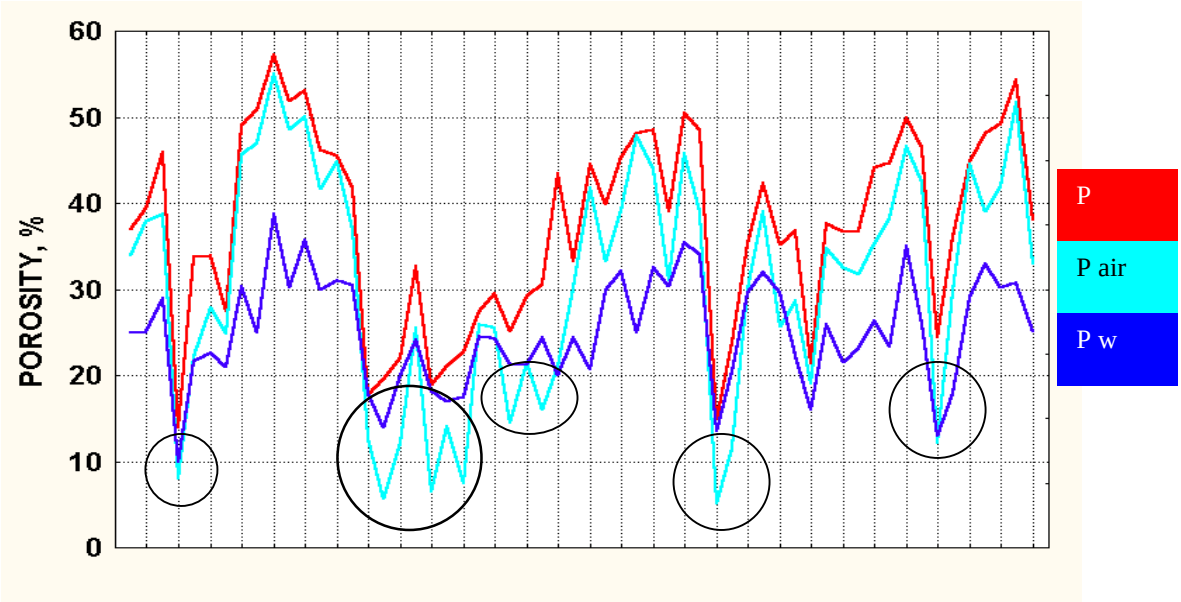

Figure 18. Line plot along sample list. Correlation of total porosity, effective porosity by air and effective porosity by water.